Progress In Electromagnetics Research M, Vol. 91, 135–142, 2020

On the EM Field Generated in the Air-Space by a Vertical Magnetic Dipole Situated on a Plane Conducting Medium

Marcello Salis[1, *] and Marco Muzi[2]

Abstract—This work presents a hybrid analytical-numerical approach to evaluate the integral representations for the time-harmonic electromagnetic (EM) field components produced in the air space by a vertical magnetic dipole (VMD) placed on a plane homogeneous conducting medium. Explicit expressions for the fields are derived by substituting a rational approximation, generated by the vector fitting algorithm, for the non-analytic part of the integrand of the electric vector potential. This permits to rewrite the representation for the electric vector potential as a combination of simple closed-contour integrals around the pole singularities of the rational approximation, which may be directly evaluated. As a result, each field component is given as a sum of cylindrical Hankel functions depending on the radial distance between source and field points, plus an exponential term that is a function of the total distance of the field point from the dipole.

1. INTRODUCTION

It is well established that information about the structure of an earthbound territory may be achieved by measuring the EM field generated by a current-carrying insulated coil of wire placed in close proximity to it [1–27]. Specifically, if the properties of the material medium do not change spatially, the nearness of shallow buried items like metals, mines, or mineral assets may be inferred from the discrepancy between the recorded measurement data and the theoretical outcomes arising from treating the soil as if it were homogeneous. In the last decades, several approaches have been proposed that allow to compute the time-harmonic EM field generated by a loop source positioned near the surface of homogeneous ground [1, 2, 4, 5, 7, 9, 28–30]. However, most of them cast the complete integral representations for the fields into forms amenable to numerical integration and, as a consequence, are typically time consuming. An attempt at developing an analytical solution to the problem has been presented in [2]. Here, the proposed explicit expressions for the fields are not subject to simplifying assumptions, but exhibit the disadvantage of being tailored to the special case where both the source loop and the observation point lie on the surface of the semi-infinite material medium. The aim of this paper is to derive new explicit expressions for the time-harmonic EM field components of a circular loop source located on a lossy ground, which are valid not only at the air side of the ground top surface, but also in the whole air-space. This feature makes it possible to overcome the restrictive hypothesis, underlying the previous approach, that the whole EM prospecting system must be situated on the soil to be explored. For the purposes of the present derivation, the loop source is regarded as a vertical magnetic dipole. This is a reasonable assumption in practical applications, as the perimeter of the loop is frequently much smaller than both the free-space wavelength and the spacing between emitter and receiver.

The field expressions are obtained starting from the integral representation for the vertical component of the electric vector potential, by replacing the non-analytic part of the integrand with

Received 20 January 2020, Accepted 9 April 2020, Scheduled 14 April 2020

* Corresponding author: Marcello Salis (marcello.salis@yahoo.it).

[1] Independent Researcher, Via Gregorio Ricci Curbastro 34, Rome 00149, Italy. [2] Department of Information Engineering, Electronics and Telecommunications, "La Sapienza" University of Rome, Via Eudossiana 18, Rome 00184, Italy.

a rational function representation according to the least squares-based vector fitting algorithm. This leads to expressing the electric vector potential as a combination of simple closed-contour integrals around the poles of the rational approximation, which may be easily analytically evaluated. As a result, the field components are given as a sum of Hankel functions depending on the radial distance between source and field points, plus an exponential function of the total distance of the field point from the dipole. Numerical tests are performed to show the validity of the developed method and its advantages in terms of time cost with respect to numerical algorithms used to evaluate Sommerfeld-type integrals.

2. THEORY

Consider a vertical magnetic dipole of moment $me^{j\omega t}$ situated at the air-side of the interface between the air and a homogeneous lossy ground, as shown in Fig. 1. The dielectric permittivity and electric conductivity of the ground are indicated with ϵ_1 and σ_1, respectively, while the magnetic permeability is assumed to be constant everywhere and equal to that of free space μ_0. Since the dipole is a magnetic point source, the electric and magnetic field vectors in the air-space ($n = 0$) and in the region occupied by the medium ($n = 1$) may be expressed in terms of an electric vector potential $\mathbf{F}$, as follows [29]

$$\mathbf{E}_n = -\boldsymbol{\nabla} \times \mathbf{F}_n, \quad \mathbf{H}_n = -(\sigma_n + j\omega\epsilon_n)\mathbf{F}_n + \frac{1}{j\omega\mu_0}\boldsymbol{\nabla}\left(\boldsymbol{\nabla} \cdot \mathbf{F}_n\right). \tag{1}$$

Because of the vertical orientation of the dipole, the scalar components of the vector Equation (1), describing the EM field components, assume a simplified form. In fact, the currents in the conducting medium flow only horizontally, and the electric field has no vertical component [29]. The electromagnetic field is thus transverse electric (TE) with respect to z, and, in virtue of the first equation in Eq. (1), the components F_x and F_y must be identically zero. As a consequence, the non-null electromagnetic field components, written in the cylindrical coordinate system (ρ, φ, z) sketched in Fig. 1, read

$$E_{\varphi_n} = \frac{\partial F_n}{\partial \rho}, \quad H_{\rho_n} = \frac{1}{j\omega\mu_0}\frac{\partial^2 F_n}{\partial\rho\partial z}, \quad H_{z_n} = -\frac{1}{j\omega\mu_0}\frac{1}{\rho}\frac{\partial}{\partial\rho}\left(\rho\frac{\partial F_n}{\partial\rho}\right), \tag{2}$$

where $F_n = F_{z_n}$ is the vertical component of the electric vector potential, which satisfies the Helmholtz equation

$$\nabla^2 F_n + k_n^2 F_n = 0. \tag{3}$$

The solution of Eq. (3) in the air space is made up of two terms, which are the primary field, excited by the source in the absence of any boundary, and the secondary (scattered) field representing the effects of the air-medium interface. For a dipole placed at the air-ground interface, it reads [29]

$$F_0 = F_p + \int_0^\infty b_0(\lambda)e^{u_0 z}J_0(\lambda\rho)d\lambda, \tag{4}$$

where the primary field F_p is given by [29, 31, 32]

$$F_p = c\frac{e^{-jk_0\sqrt{\rho^2+z^2}}}{\sqrt{\rho^2+z^2}} = c\int_0^\infty \frac{e^{-u_0|z|}}{u_0}J_0(\lambda\rho)\lambda d\lambda, \tag{5}$$

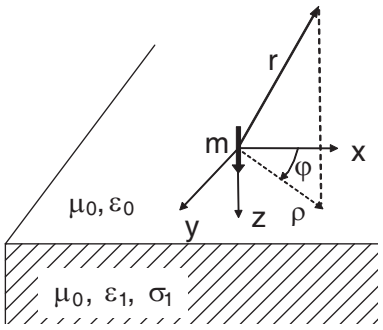

Figure 1. Sketch of a vertical magnetic dipole on a homogeneous ground.

with $u_n = \sqrt{\lambda^2 - k_n^2}$, $k_n^2 = \omega^2\mu_0\epsilon_n - j\omega\mu_0\sigma_n$, $c = j\omega\mu_0 m/(4\pi)$, and $J_0(\cdot)$ being the zeroth-order Bessel function. On the other hand, since the ground is not lower bounded, the fields here can only propagate downwards. Hence, the electric potential in the material medium may be expressed as

$$F_1 = \int_0^\infty a_1(\lambda) e^{-u_1 z} J_0(\lambda\rho)\, d\lambda \tag{6}$$

where the unknown function $a_1(\lambda)$, as well as $b_0(\lambda)$, may be determined by imposing the continuity of the tangential electric and magnetic fields across the interface at $z = 0$. This leads to the identities

$$F_0|_{z=0^-} = F_1|_{z=0^+}, \quad \left.\frac{\partial F_0}{\partial z}\right|_{z=0^-} = \left.\frac{\partial F_1}{\partial z}\right|_{z=0^+}, \tag{7}$$

which, after substituting Eqs. (4) and (6), may be solved for b_0 to give

$$b_0 = c\frac{\lambda}{u_0}\frac{u_0 - u_1}{u_0 + u_1}. \tag{8}$$

As a consequence, Equation (4) for the total electric vector potential in the air space ($z \le 0$) is turned into

$$F_0 = c\int_0^\infty \left[e^{-u_0|z|} + \frac{u_0 - u_1}{u_0 + u_1} e^{u_0 z}\right] \frac{\lambda}{u_0} J_0(\lambda\rho) d\lambda = 2c\int_0^\infty \frac{e^{u_0 z}}{u_0 + u_1} J_0(\lambda\rho)\lambda\, d\lambda. \tag{9}$$

The purpose of this work is to derive explicit formulas for the EM field components produced above the ground. The task may be accomplished by evaluating the integral representations for F_0 and its first-order z-derivative, and then substituting the obtained expressions into the right-hand sides of (2). To evaluate F_0, we first multiply the numerator and denominator of the fraction of the integrand in Eq. (9) by $u_0 - u_1$, so as to obtain

$$F_0 = \frac{j\omega\mu_0 m}{2\pi(k_1^2 - k_0^2)}\left[\int_0^\infty u_0 e^{u_0 z} J_0(\lambda\rho)\lambda\, d\lambda - \int_0^\infty u_1 e^{u_0 z} J_0(\lambda\rho)\lambda\, d\lambda\right] = \frac{j\omega\mu_0 m}{2\pi(k_1^2 - k_0^2)}(S_0 - S_1), \tag{10}$$

and notice that the integral S_0 has an explicit form, since it is related to Eq. (5). In fact, it is found that

$$S_0 = \frac{\partial^2}{\partial z^2}\int_0^\infty \frac{e^{u_0 z}}{u_0} J_0(\lambda\rho)\lambda\, d\lambda = \frac{\partial^2}{\partial z^2}\left(\frac{e^{-jk_0 r}}{r}\right) = \left[-r^2(1 + jk_0 r) + z^2(3 + 3jk_0 r - k_0^2 r^2)\right]\frac{e^{-jk_0 r}}{r^5}, \tag{11}$$

with $r = \sqrt{\rho^2 + z^2}$. On the other hand, to evaluate S_1 it suffices to extend its range of integration to the negative real axis. This may be done through substitution of the identity [8, 33]

$$J_0(\lambda\rho) = \frac{1}{2}\left[H_0^{(2)}(\lambda\rho) - H_0^{(2)}(\bar{\lambda}\rho)\right], \tag{12}$$

where $\bar{\lambda} = \lambda\exp(-j\pi)$ and $H_0^{(2)}(\cdot)$ is the zeroth-order Hankel function of the second kind. It yields

$$\begin{aligned} S_1 &= \frac{1}{2}\left\{\int_0^\infty u_1(\lambda) e^{u_0(\lambda) z} H_0^{(2)}(\lambda\rho)\lambda d\lambda - \int_0^{\infty e^{-j\pi}} u_1(\bar{\lambda}) e^{u_0(\bar{\lambda}) z} H_0^{(2)}(\bar{\lambda}\rho)\bar{\lambda} d\bar{\lambda}\right\} \\ &= \frac{1}{2}\int_{\infty e^{-j\pi}}^\infty u_1 e^{u_0 z} H_0^{(2)}(\lambda\rho)\lambda d\lambda, \end{aligned} \tag{13}$$

where the final contour of integration consists of the lower shore of the negative real λ-axis and the positive real λ-axis. The idea now is to replace the non-analytic part of the integrand in Eq. (13) with an accurate rational approximation in pole-residue form. In order to perform this task with maximum efficiency, the function to be approximated must be chosen so that it decays as quickly as possible as λ is increased. Hence, it is convenient to move the factor u_1 of the integrand to the denominator. To this goal, we rewrite Eq. (13) as follows

$$S_1 = \frac{1}{2}\int_{\infty\, e^{-j\pi}}^\infty \frac{\lambda^2 - k_1^2}{u_1} e^{u_0 z} H_0^{(2)}(\lambda\rho)\lambda\, d\lambda. \tag{14}$$

Then, application of the least squares-based fitting algorithm proposed in [34] allows to obtain the following rational approximation in terms of partial fractions

$$\frac{e^{u_0 z}}{u_1} \cong \sum_{l=1}^{L} \frac{r_l}{j\lambda^2 - p_l}, \quad \mathrm{Re}\,[p_l] < 0, \tag{15}$$

where L is the order of the approximation. Performing the substitution of Eq. (15) permits to deform the contour of integration to a new path, constituted by the lower infinite semi-circle and a set of circles, the latter enclosing the poles of the sum of partial fractions in Eq. (15) that lie in the lower half of the complex λ-plane. Since the integrand vanishes as $|\lambda|$ is increased in the lower half of the complex plane, it is concluded that the infinite semi-circle does not contribute to the contour integral, and Eq. (14) is simplified to

$$S_1 = -\frac{j}{2} \sum_{l=1}^{L} r_l \int_{C_l} \frac{\lambda^2 - k_1^2}{\lambda^2 + jp_l} H_0^{(2)}(\lambda\rho)\lambda \, d\lambda \tag{16}$$

C_l is the infinitesimal circumference surrounding the pole $\lambda_l = -\sqrt{-jp_l}$, lying on the lower half of the complex λ-plane. The lth integral along the circle C_l can thus be evaluated analytically through application of Cauchy's integral formula. It yields

$$\int_{C_l} \frac{\lambda^2 - k_1^2}{\lambda^2 + jp_l} H_0^{(2)}(\lambda\rho)\lambda \, d\lambda = -2\pi j \lim_{\lambda \to \lambda_l} (\lambda - \lambda_l) \frac{\lambda^2 - k_1^2}{\lambda^2 - \lambda_l^2} H_0^{(2)}(\lambda\rho)\lambda = -\pi j(\lambda_l^2 - k_1^2) H_0^{(2)}(\lambda_l\rho), \tag{17}$$

hence, the integral S_1 in Eq. (16) assumes the explicit form

$$S_1 = -\frac{\pi}{2} \sum_{l=1}^{L} r_l \left(\lambda_l^2 - k_1^2\right) H_0^{(2)}(\lambda_l\rho), \tag{18}$$

which may be substituted together with Eq. (11) into Eq. (10) to give

$$F_0 = \frac{j\omega\mu_0 m}{2\pi(k_1^2 - k_0^2)} \left\{ \left[-r^2(1 + jk_0 r) + z^2(3 + 3jk_0 r - k_0^2 r^2)\right] \frac{e^{-jk_0 r}}{r^5} + \frac{\pi}{2} \sum_{l=1}^{L} r_l \left(\lambda_l^2 - k_1^2\right) H_0^{(2)}(\lambda_l\rho) \right\}. \tag{19}$$

Analogously, an explicit formula for the first-order z-derivative of F_0 may also be derived. In fact, from Eq. (10) it follows that

$$\frac{\partial F_0}{\partial z} = \frac{j\omega\mu_0 m}{2\pi(k_1^2 - k_0^2)} \left\{ \left[3r^2(3 + 3jk_0 r - k_0^2 r^2) - z^2(15 + 15jk_0 r - 6k_0^2 r^2 - jk_0^3 r^3)\right] \frac{ze^{-jk_0 r}}{r^7} - \frac{\partial S_1}{\partial z} \right\}, \tag{20}$$

where the z-derivative of S_1 may be obtained from Eq. (18) by multiplying the lth term on the right-hand side by $u_0(\lambda_l) = \sqrt{\lambda_l^2 - k_0^2}$, since $\partial e^{u_0 z}/\partial z = u_0 e^{u_0 z}$. Hence, the z-derivative of S_1 assumes the form

$$\frac{\partial S_1}{\partial z} = -\frac{\pi}{2} \sum_{l=1}^{L} r_l \sqrt{\lambda_l^2 - k_0^2} \left(\lambda_l^2 - k_1^2\right) H_0^{(2)}(\lambda_l\rho), \tag{21}$$

which, used together with Eqs. (20) and (19) in Eq. (2), leads to the explicit expressions for the electromagnetic field components in air, namely

$$E_{\varphi_0} = \frac{j\omega\mu_0 m}{2\pi(k_1^2 - k_0^2)} \left\{ \left[r^2(3 + 3jk_0 r - k_0^2 r^2) - z^2(15 + 15jk_0 r - 6k_0^2 r^2 - jk_0^3 r^3)\right] \frac{\rho\, e^{-jk_0 r}}{r^7} \right.$$
$$\left. - \frac{\pi}{2} \sum_{l=1}^{L} r_l \lambda_l \left(\lambda_l^2 - k_1^2\right) H_1^{(2)}(\lambda_l\rho) \right\}, \tag{22}$$

$$H_{\rho_0} = \frac{m}{2\pi(k_1^2 - k_0^2)} \left\{ \left[-3r^2(15 + 15jk_0 r - 6k_0^2 r^2 - jk_0^3 r^3) + z^2(105 + 105jk_0 r - 45k_0^2 r^2 - 10jk_0^3 r^3 + k_0^4 r^4)\right] \right.$$
$$\left. \times \frac{\rho z e^{-jk_0 r}}{r^9} - \frac{\pi}{2} \sum_{l=1}^{L} r_l \lambda_l \sqrt{\lambda_l^2 - k_0^2} \left(\lambda_l^2 - k_1^2\right) H_1^{(2)}(\lambda_l\rho) \right\}, \tag{23}$$

$$H_{z_0} = \frac{m}{2\pi(k_1^2 - k_0^2)} \left\{ \left[r^4(9 + 9jk_0r - 4k_0^2r^2 - jk_0^3r^3) + r^2z^2(-90 - 90jk_0r + 39k_0^2r^2 + 9jk_0^3r^3 - k_0^4r^4) \right.\right.$$
$$\left.\left. + z^4(105 + 105jk_0r - 45k_0^2r^2 - 10jk_0^3r^3 + k_0^4r^4) \right] \frac{e^{-jk_0r}}{r^9} + \frac{\pi}{2} \sum_{l=1}^{L} r_l \lambda_l^2 \left(\lambda_l^2 - k_1^2\right) H_0^{(2)}(\lambda_l \rho) \right\} \quad (24)$$

3. VALIDATION OF THE FORMULATION

As validation of the theoretical development, Equation (24) is used to calculate the vertical magnetic field component that a dipole with moment $m = 1\,\mathrm{A}\cdot\mathrm{m}^2$ produces at a plane 1 m apart from the interface between air and a clay soil, with $\sigma_1 = 10\,\mathrm{mS/m}$ and $\epsilon_1 = 10\,\epsilon_0$ [10]. At first, the H_z-field is computed against the radial distance ρ between the source and field points, assuming that the operating frequency is equal to 10 kHz. The length chosen for the sum of partial fractions in Eq. (15) is $L = 10$, and the poles and residues are determined through an iterative process which consists of repeatedly applying the fitting procedure in [34], until the root mean square relative error of the approximation of Eq. (15) falls below the tolerable error of 10^{-4}. The process is started by assuming that the guess values for the poles of the approximation are $p_l = (-1 + jq_l)\,\mathrm{m}^{-2}$ $(l = 1, 2, \ldots, 10)$, with the q_l's linearly distributed in the interval $[-15, 15]$. With the above assumptions, the iterative process terminates after 16 iterations, when the RMS relative error of the approximation of Eq. (15) with $L = 10$ is slightly more than 10^{-7}. The corresponding ρ-profile provided by Eq. (24) is shown in Fig. 2, which also illustrates the trends associated with lower-order rational approximations, as well as the results arising from numerically evaluating the integral representation for H_z, which comes from substituting Eq. (9) into the last of Equation (2). Numerical integration is carried out through a Gauss-Kronrod G7-K15 scheme, originating from the combination of a 7-point Gauss rule with a 15-point Kronrod rule. From the analysis of the plotted curves it emerges that increasing the order of the rational approximation L improves the accuracy of the result of the computation. In fact, if L grows up the curves provided by Eq. (24) approach the outcomes from numerical quadrature, and when $L = 10$ excellent agreement is achieved as expected. Thus, the proposed series-form approximate solution converges to the exact solution. This is confirmed by the curves plotted in Fig. 3, which shows the relative error of the outcomes from Eq. (24) as compared to numerical integration data. As seen, except for large values of ρ, the error monotonically decreases as L is increased. On the other hand, when ρ is large, the error quickly drops with increasing L only if L is also sufficiently large.

Thus, the accuracy of the result of the computation significantly depends on the value of ρ, and in particular, Fig. 3 shows that for a given value of L the relative error may vary by three orders of magnitude within the considered ρ-interval. Significant variations in accuracy are instead not observed while changing the electrical conductivity σ_1 of the lossy ground. This aspect is illustrated by Figs. 4

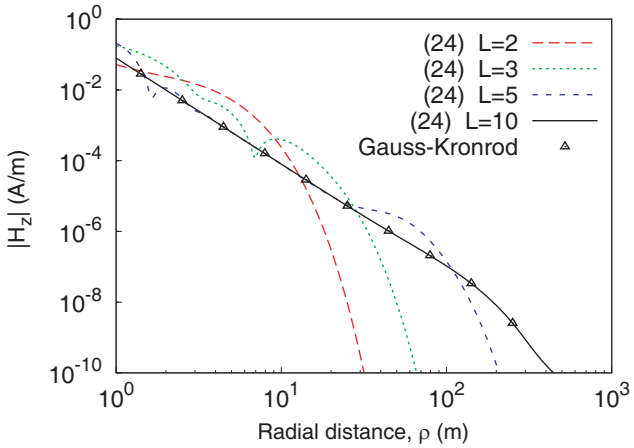

Figure 2. Amplitude of H_z against the radial distance from the source point.

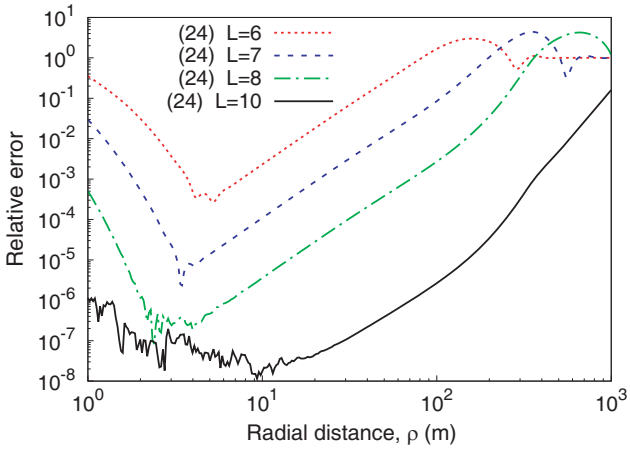

Figure 3. Relative error of (24) as compared to G7-K15 scheme, plotted against ρ.

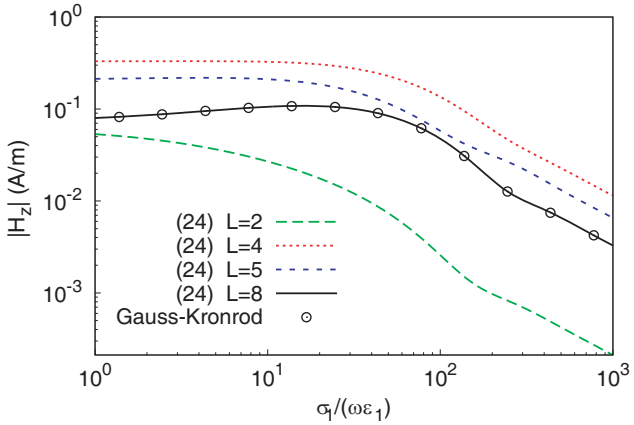

Figure 4. Amplitude of H_z against the normalized conductivity of the ground $\sigma_1/(\omega\epsilon_1)$.

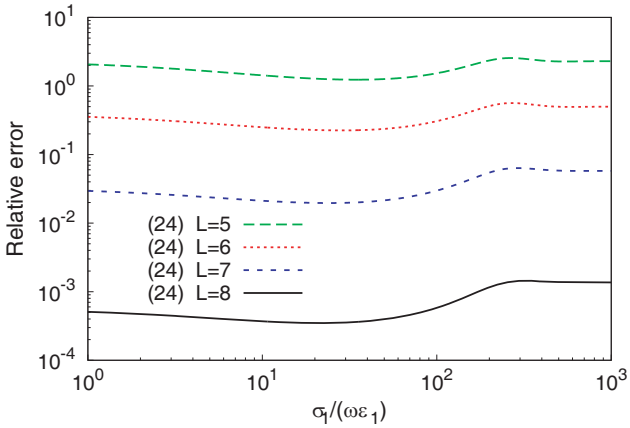

Figure 5. Relative error of (24) as compared to G7-K15 scheme, plotted against $\sigma_1/(\omega\epsilon_1)$.

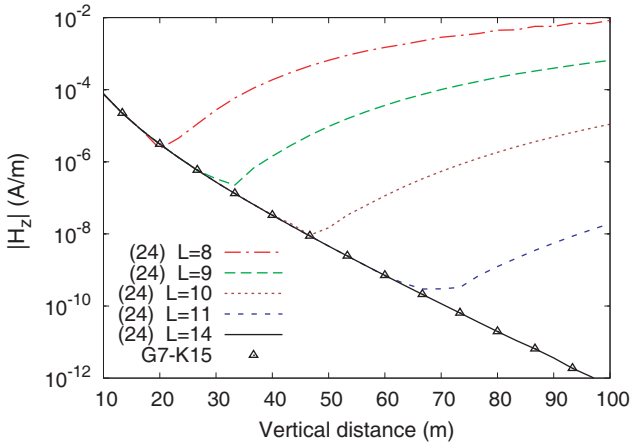

Figure 6. Profiles of $|H_z|$ against the vertical distance from the source point.

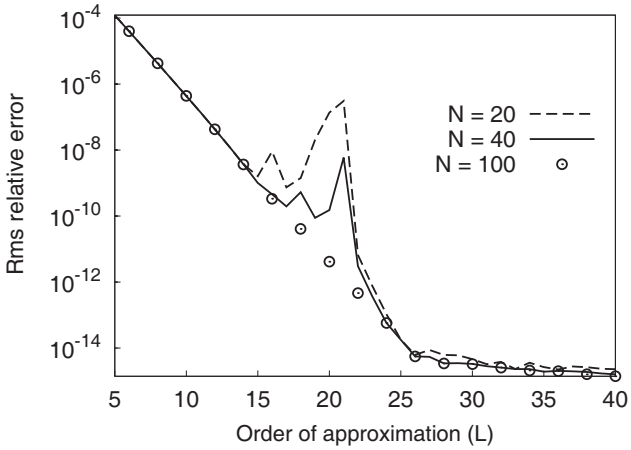

Figure 7. RMS relative error of the approximation in (15) against the number of terms L.

and 5, which show, respectively, profiles of $|H_z|$ versus the ratio $\sigma_1/(\omega\epsilon_1)$, and the relative error resulting from using Eq. (24) instead of G7-K15 scheme. Here, it is assumed that the source is a unit-moment dipole which operates at 10 MHz, and that $\epsilon_1 = 10\epsilon_0$, $\rho = 1\,\text{m}$, and $z = -50\,\text{cm}$. Fig. 4 tells us that the sequence of trends generated by the partial sums in Eq. (24) converges to the profile provided by the G7-K15 scheme, and that excellent agreement is achieved starting from $L = 8$. On the other hand, a glance at the curves plotted in Fig. 5 leads to the conclusion that the error by the outcomes from the proposed approach weakly depends on the normalized conductivity $\sigma_1/(\omega\epsilon_1)$. In the good-conductor limit ($\sigma_1 \gg \omega\epsilon_1$), the error is not affected by conductivity changes. One might ask how changing the vertical distance of the field point from the air-ground interface affects the accuracy of the outcomes from the proposed approach. This aspect is illustrated by Fig. 6, which shows z-profiles of the H_z-field strength corresponding to distinct values of L, calculated by assuming that the unit-moment dipole still operates at 10 MHz, and that $\sigma_1 = 1\,\text{mS/m}$, $\epsilon_1 = 10\epsilon_0$, and $\rho = 2\,\text{m}$. The plotted curves clearly point out that, as the vertical distance grows up, the length of the sum in Eq. (15) must be progressively, although moderately, increased in order to maintain a good level of accuracy. As previously anticipated, for a fixed value of L application of the fitting algorithm in [34] has been iterated until the RMS relative error of Eq. (15) falls below a specified threshold. However, the relative error is lower bounded, and it cannot be decreased as much as desired. This point is clarified by Fig. 7, which depicts, for a wide set of values of L, the error achievable by repeating the execution of the fitting process N times, with N

taken as a parameter. The electromagnetic and geometric parameters are the same as those assumed in the example of Fig. 2. As seen, the number of iterations required to reach the lower limit of the error strongly depends on L, and it is smaller when L is small or large. For intermediate values of L, about 100 iterations are required in order to approach the minimum error. On the other hand, the minimum achievable error decreases with increasing L, and for $L > 25$ about 20 iterations are enough to achieve an RMS relative error smaller than 10^{-14}.

With accuracy being equal, the proposed method makes it possible to save computation time compared to G7-K15 numerical scheme. In fact, the average CPU time taken by Eq. (24) to generate the profile of $|H_z|$ associated with $L = 8$ in Fig. 4 is equal to 1.57 ms, while about 9 s are taken by numerical integration to produce the same outcome. This means that the speed-up offered by Eq. (24), which is the ratio of the time taken by Gaussian integration to that required by the proposed approach, about $5.7 \cdot 10^3$.

4. CONCLUSIONS

This paper has presented an efficient hybrid analytical-numerical approach for evaluating the integral expressions for the EM field components generated in the air space by a vertical magnetic dipole placed on a homogeneous earth. The approach consists of deriving explicit expressions for the field, by replacing the non-oscillating-part of the integrand of the electric vector potential with a rational approximation arising from applying a least squares-based fitting algorithm. This leads to turning the integral representation for the electric vector potential into a sum of closed-contour integrals about the poles of the rational function, which may be easily evaluated. The proposed method is useful in practical applications like, for instance, electromagnetic sounding technique for ground exploration. In such a context, it may be integrated in the signal or data processing unit of measurement/testing devices.

REFERENCES

1. Zhdanov, M. S., *Geophysical Electromagnetic Theory and Methods*, Elsevier, Amsterdam, 2009.
2. Parise, M., "An exact series representation for the EM field from a circular loop antenna on a lossy half-space," *IEEE Antennas and Wireless Propagation Letters*, Vol. 13, 23–26, 2014.
3. Farquharson, C. G., D. W. Oldenburg, and P. S. Routh, "Simultaneous 1D inversion of loop-loop electromagnetic data for magnetic susceptibility and electrical conductivity," *Geophysics*, Vol. 68, No. 6, 1857–1869, 2003.
4. Parise, M., "Efficient computation of the surface fields of a horizontal magnetic dipole located at the air-ground interface," *International Journal of Numerical Modelling: Electronic Networks, Devices and Fields*, Vol. 29, 653–664, 2016.
5. Wait, J. R., "Mutual electromagnetic coupling of loops over a homogeneous ground," *Geophysics*, Vol. 20, No. 3, 630–637, 1955.
6. Beard, L. P. and J. E. Nyquist, "Simultaneous inversion of airborne electromagnetic data for resistivity and magnetic permeability," *Geophysics*, Vol. 63, No. 5, 1556–1564, 1998.
7. Spies, B. R. and F. C. Frischknecht, "Electromagnetic sounding," *Electromagnetic Methods in Applied Geophysics, Volume 2*, M. N. Nabighian, Ed., 285–426, SEG, Tulsa, Oklahoma, 1988.
8. Parise, M., "Exact EM field excited by a short horizontal wire antenna lying on a conducting soil," *AEU — International Journal of Electronics and Communications*, Vol. 70, No. 5, 676–680, 2016.
9. Telford, W. M., L. P. Geldart, and R. E. Sheriff, *Applied Geophysics*, Cambridge University Press, New York, 1990.
10. Palacky, G. J., "Resistivity characteristics of geologic targets," *Electromagnetic Methods in Applied Geophysics*, Nabighian, M. N., Ed., Vol. 1, 52–129, SEG, Tulsa, Oklahoma, 1988.
11. Parise, M., "Full-wave analytical explicit expressions for the surface fields of an electrically large horizontal circular loop antenna placed on a layered ground," *IET Microwaves, Antennas & Propagation*, Vol. 11, 929–934, 2017.

12. Parise, M., "On the surface fields of a small circular loop antenna placed on plane stratified earth," *International Journal of Antennas and Propagation*, Vol. 2015, 1–8, 2015.
13. Singh, N. P. and T. Mogi, "Electromagnetic response of a large circular loop source on a layered earth: A new computation method," *Pure and Applied Geophysics*, Vol. 162, 181–200, 2005.
14. Chew, W. C., *Waves and Fields in Inhomogeneous Media*, IEEE Press, Piscataway, NJ, 1995.
15. Parise, M. and G. Antonini, "On the inductive coupling between two parallel thin-wire circular loop antennas," *IEEE Transactions on Electromagnetic Compatibility*, Vol. 60, 1865–1872, 2018.
16. Wait, J. R., "Fields of a horizontal loop antenna over a layered half-space," *Journal of Electromagnetic Waves and Applications*, Vol. 9, 1301–1311, 1995.
17. Parise, M., "A study on energetic efficiency of coil antennas used for RF diathermy," *IEEE Antennas and Wireless Propagation Letters*, Vol. 10, 385–388, 2011.
18. Singh, N. P. and T. Mogi, "EMLCLLER-A program for computing the EM response of a large loop source over a layered earth model," *Computer and Geosciences*, Vol. 29, No. 10, 1301–1307, 2003.
19. Parise, M., V. Tamburrelli, and G. Antonini, "Mutual impedance of thin-wire circular loops in near-surface applications," *IEEE Transactions on Electromagnetic Compatibility*, Vol. 61, 558–563, 2019.
20. Shastri, N. L. and H. P. Patra, "Multifrequency sounding results of laboratory simulated homogeneous and two-Layer earth models," *IEEE Trans. Geosci. Remote Sensing*, Vol. 26, No. 6, 749–752, 1988.
21. Parise, M., "Fast computation of the forward solution in controlled-source electromagnetic sounding problems," *Progress In Electromagnetics Research*, Vol. 111, 119–139, 2011.
22. Kong, J. A., L. Tsang, and G. Simmons, "Geophysical subsurface probing with radio-frequency interferometry," *IEEE Transactions on Antennas and Propagation*, Vol. 22, No. 4, 616–620, 1974.
23. Singh, N. P. and T. Mogi, "Inversion of large loop transient electromagnetic data over layered earth models," *Jour. Fac. Sci Hokkaido Univ. Ser. VII*, Vol. 12, No. 1, 41–54, 2003.
24. Parise, M., "On the use of cloverleaf coils to induce therapeutic heating in tissues," *Journal of Electromagnetic Waves and Applications*, Vol. 25, 1667–1677, 2011.
25. Parise, M., "Improved Babylonian square root algorithm-based analytical expressions for the surface-to-surface solution to the Sommerfeld half-space problem," *IEEE Transactions on Antennas and Propagation*, Vol. 63, 5832–5837, 2015.
26. Simons, N. R. S., A. Sebak, and G. E. Bridges, "Application of the TLM method to half-space and remote-sensing problems," *IEEE Trans. Geosci. Remote Sensing*, Vol. 33, No. 3, 759–767, 1995.
27. Singh, D., N. K. Choudhary, K. C. Tiwari, and R. Prasad, "Shape recognition of shallow buried metallic objects at x-band using ann and image analysis techniques," *Progress In Electromagnetics Research B*, Vol. 13, 257–273, 2009.
28. Parise, M., "Quasi-static vertical magnetic field of a large horizontal circular loop located at the earth's surface," *Progress In Electromagnetics Research Letters*, Vol. 62, 29–34, 2016.
29. Ward, S. H. and G. W. Hohmann, "Electromagnetic theory for geophysical applications," *Electromagnetic Methods in Applied Geophysics, Theory — Volume 1*, M. N. Nabighian (ed.), 131–308, SEG, Tulsa, Oklahoma, 1988.
30. Kong, J. A., *Electromagnetic Wave Theory*, John Wiley & Sons, New York, 1986.
31. Parise, M., "Second-order formulation for the quasi-static field from a vertical electric dipole on a lossy half-space," *Progress In Electromagnetics Research*, Vol. 136, 509–521, 2013.
32. Parise, M., "A highly accurate analytical solution for the surface fields of a short vertical wire antenna lying on a multilayer ground," *Waves in Random and Complex Media*, Vol. 28, 49–59, 2018.
33. Parise, M., "An exact series representation for the EM field from a vertical electric dipole on an imperfectly conducting half-space," *Journal of Electromagnetic Waves and Applications*, Vol. 28, 932–942, 2014.
34. Gustavsen, B. and A. Semlyen, "Rational approximation of frequency domain responses by vector fitting," *IEEE Trans. Power Delivery*, Vol. 14, No. 3, 1052–1061, 1999.